PHYSICAL REVIEW D **75,** 054021 (2007)

$pp \to pp\eta'$ reaction at high energies

A. Szczurek*

Institute of Nuclear Physics PAN, PL-31-342 Cracow, Poland and University of Rzeszów, PL-35-959 Rzeszów, Poland

R. S. Pasechnik† and O. V. Teryaev‡

Bogoliubov Laboratory of Theoretical Physics, JINR, Dubna 141980, Russia
and Faculty of Physics, Moscow State University, Moscow 119992, Russia

(Received 19 September 2006; published 16 March 2007)

We discuss double-diffractive (double-elastic) production of the η'-meson in the $pp \to p\eta' p$ reaction within the formalism of unintegrated gluon distribution functions (UGDF). We estimate also the contribution of $\gamma^*\gamma^* \to \eta'$ fusion. The distributions in the Feynman x_F (or rapidity), transferred four-momenta squared between initial and final protons (t_1, t_2) and azimuthal angle difference between outgoing protons (Φ) are calculated. The deviations from the $\sin^2(\Phi)$ dependence predicted by one-step vector-vector-pseudoscalar coupling are quantified and discussed. The results are compared with the results of the WA102 collaboration at CERN. Most of the models of UGDF from the literature give a too small cross section as compared to the WA102 data and predict angular distribution in relative azimuthal angle strongly asymmetric with respect to $\pi/2$ in disagreement with the WA102 data. This points to a different mechanism at the WA102 energy. Predictions for RHIC, Tevatron and LHC are given. We find that the normalization, $t_{1,2}$ dependences as well as deviations from $\sin^2(\Phi)$ of double-diffractive double-elastic cross section are extremely sensitive to the choice of UGDF. Possible implications for UGDFs are discussed.

DOI: 10.1103/PhysRevD.75.054021 PACS numbers: 13.87.Ce, 13.60.Le, 13.85.Lg

I. INTRODUCTION

The search for Higgs boson is the primary task for the LHC collider being now constructed at CERN. Although the predicted cross section is not small it may not be easy to discover Higgs in inclusive reaction due to large background in each of the final channels considered. An alternative way [1–3] is to search for Higgs in exclusive or semiexclusive reactions with large rapidity gaps. Although the cross section is not large, the ratio of the signal to more conventional background seems promising. Kaidalov, Khoze, Martin and Ryskin proposed to calculate diffractive double-elastic[1] production of Higgs boson in terms of unintegrated gluon distributions [4–7]. It is not clear at present how reliable such calculations are. It would be very useful to use the formalism to a reaction which is easy to measure. Here we shall try to apply it to the production of η' meson which satisfies this criterion.

Recently the exclusive production of η' meson in proton-proton collisions was intensively studied slightly above its production threshold at the COSY ring at KFA Jülich [8] and at Saclay [9]. Here the dominant production mechanism is exchange of several mesons (so-called meson exchange currents) and reaction via S_{11} resonance [10].

In the present paper we study the same exclusive channel but at much larger energies ($W > 10$ GeV). Here diffractive mechanism is expected to be the dominant process. In Ref. [11] the Regge-inspired pomeron-pomeron fusion was considered as the dominant mechanism of the η' production.

There is a long standing debate about the nature of the pomeron. The approximate $\sin^2(\Phi)$ (Φ is the azimuthal angle between outgoing protons) dependence observed experimentally [12] was interpreted in Ref. [13] as due to (vector pomeron)-(vector pomeron)-(pseudoscalar meson) coupling. To our knowledge no QCD-inspired calculation for diffractive production of pseudoscalar mesons exists in the literature.

Of course, one should worry about the origin of the hard scale which may justify the applicability of QCD perturbation theory. As soon as the mass of η' is not sufficient for that, it can be reasonably large η' transverse momentum (or $t_{1,2}$) which would serve as a hard scale. Bearing this in mind, we will examine the QCD result in the whole kinematical region, which should be understood as a sort of continuation of perturbative result to the region where its applicability cannot be rigorously proven.

In Fig. 1 we show the QCD mechanism of diffractive double-elastic production of η' meson, analogous to the mechanism of Higgs boson production. We shall show here that approximate ($\sim \sin^2(\Phi)$) dependence is violated in the QCD-inspired model with gluon exchanges within the formalism of unintegrated gluon distribution functions (UGDF) and a distortion from this dependence can help to select the correct model of UGDF. For completeness, in this paper we shall include photon-photon fusion mechanism shown in Fig. 2 which was sometimes advocated as dominant mechanism at high energies.

*Electronic address: antoni.szczurek@ifj.edu.pl
†Electronic address: rpasech@theor.jinr.ru
‡Electronic address: teryaev@theor.jinr.ru
[1]Both protons survive the collision.

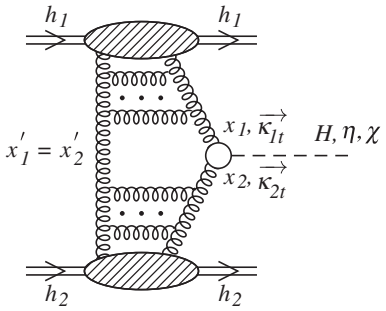

FIG. 1. The sketch of the bare QCD mechanism. The kinematical variables are shown in addition.

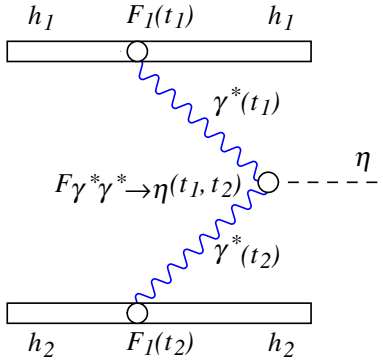

FIG. 2 (color online). The sketch of the photon-photon fusion mechanism. Form factors appearing in different vertices are shown explicitly.

II. FORMALISM

A. Diffractive QCD mechanism

The kinematics of the process on the quark level is shown in Fig. 3. The decomposition of gluon momenta into longitudinal and transverse parts gives

$$\begin{aligned} k_0 &= -x_1' p_1 + k_{0,t} = x_2' p_2 + k_{0,t}, \\ k_1 &= x_1(k_0 - p_1) + k_{1,t}, \\ k_2 &= x_2(p_2 + k_0) + k_{2,t}. \end{aligned} \tag{2.1}$$

We take into account below that $x_1' = x_2' = x_0$. Making use of conservation laws we get

$$k_1 + p_1' = p_1 - k_0, \qquad k_2 + p_2 + k_0 = p_2'. \tag{2.2}$$

Taking the transverse parts from these relations gives

$$k_{1,t} = -(p_{1,t}' + k_{0,t}), \qquad k_{2,t} = p_{2,t}' - k_{0,t}. \tag{2.3}$$

Following the formalism for the diffractive double-elastic production of the Higgs boson developed by Kaidalov, Khoze, Martin and Ryskin [4–7] (KKMR) we write the bare QCD amplitude for the process sketched in Fig. 1 as[2]

$$\mathcal{M}^{g^*g^*\to\eta'}_{pp\to p\eta' p} = i\pi^2 \int d^2k_{0,t} V(k_1, k_2, P_M) \frac{f^{\rm off}_{g,1}(x_1, x_1', k_{0,t}^2, k_{1,t}^2, t_1) f^{\rm off}_{g,2}(x_2, x_2', k_{0,t}^2, k_{2,t}^2, t_2)}{k_{0,t}^2 k_{1,t}^2 k_{2,t}^2}. \tag{2.4}$$

The normalization of this amplitude differs from the KKMR one [5,15] by the factor i. The bare amplitude above is subjected to absorption corrections which depend on collision energy. We shall discuss this issue shortly when presenting our results.

The vertex function $V(k_1, k_2, P_M)$ in the expression (2.4) describes the coupling of two virtual gluons to the pseudoscalar meson. We take the gluon-gluon-pseudoscalar meson coupling in the form

$$V_{\alpha\beta}(k_1, k_2, P_M) = V_N F_{g^*g^*\to\eta'}(k_1^2, k_2^2) \varepsilon_{\mu\nu\alpha\beta} k_1^\mu k_2^\nu. \tag{2.5}$$

Normalization is such that $F_{g^*g^*\to\eta'}(0, 0) = 1$. The normalization constant V_N can be obtained in terms of the partial decay width $\Gamma(\eta' \to gg)$ as

$$V_N^2 = K \frac{64\pi\Gamma(\eta' \to gg)}{(N_c^2 - 1) m_{\eta'}^3}, \qquad \text{NLO} \to K = 1.5. \tag{2.6}$$

The same normalization was obtained for the QCD double-diffractive production of χ mesons in [15].

The gauge invariance requires $k_1^\alpha V_{\alpha\beta} = k_2^\beta V_{\alpha\beta} = 0$. On the parton level using Feynman rules we have to "hook" the gluon-gluon-pseudoscalar meson coupling (2.5) to the quark line by contracting it with incoming quark momenta. Replacing the quark lines by the proton lines one can show that the vertex factor $V(k_1, k_2, P_M)$ in the amplitude (2.4) has the following form

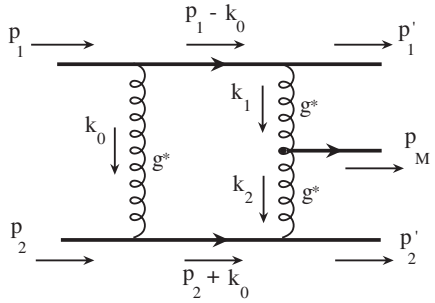

FIG. 3. Kinematics of exclusive double-diffractive η'-meson production.

[2]For a sketchy derivation of this formula starting from the parton level one may look to [14].

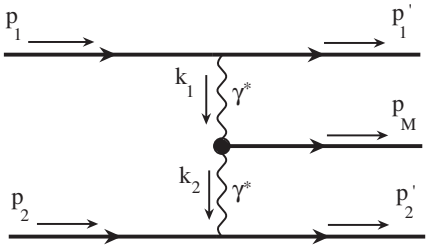

FIG. 4. Kinematics of exclusive $\gamma^*\gamma^*$ fusion mechanism of η'-meson production.

$$V = (k_0 - p_1)^\alpha (p_2 + k_0)^\beta V_{\alpha\beta} = \frac{k^\alpha_{1,t}}{x_1}\frac{k^\beta_{2,t}}{x_2} V_{\alpha\beta}. \quad (2.7)$$

Using relations (2.1), (2.3), and (2.5) this expression can be transformed to

$$V = V_N F_{g^*g^*\to\eta'}(k_1^2, k_2^2)\varepsilon_{\mu\nu\alpha\beta}(p_1 + p_2)^\mu (p_2 + k_0)^\nu \times (p'_{1,t} + k_{0,t})^\alpha (p'_{2,t} - k_{0,t})^\beta.$$

In the c.m.s. system $\mathbf{p_1} + \mathbf{p_2} = 0$ and $(p_1 + p_2)_0 = \sqrt{s}$. Since $\mathbf{k}_{0,t} \perp [\mathbf{p}'_{1,t} \times \mathbf{p}'_{2,t}]$ we have

$$V = -V_N\sqrt{s}F_{g^*g^*\to\eta'}(k_1^2, k_2^2)\varepsilon_{ikl}(p'_{1,t} + k_{0,t})_i \times (p'_{2,t} - k_{0,t})_k p_{1,l}. \quad (2.8)$$

Introducing a unit vector in the beam direction of ingoing protons in c.m.s. $n_l = p_{1,l}/|\mathbf{p}_1|$, we get finally

$$V = -V_N\frac{s}{2}F_{g^*g^*\to\eta'}(k_1^2, k_2^2)[(\mathbf{p}'_{1,t} + \mathbf{k}_{0,t}) \times (\mathbf{p}'_{2,t} - \mathbf{k}_{0,t})]\mathbf{n}. \quad (2.9)$$

Normalization of this vertex function differs from the KKMR one [5,15] by the factor $sF_{g^*g^*\to\eta'}/2$. Form factor $F_{g^*g^*\to\eta'}$ can be relevant at some kinematical regions and it should be taken into account. Factor $s/2$ makes the normalization of the full bare QCD amplitude (2.4) consistent with canonical normalization of the cross section (see Eq. (2.29)).

Expression (2.8) can be also written as

$$V(k_1, k_2, P_M) = V_N\frac{s}{2}F_{g^*g^*\to\eta'}(k_1^2, k_2^2)\cdot|\mathbf{k}_{1,t}||\mathbf{k}_{2,t}|\cdot\sin(\phi), \quad (2.10)$$

where ϕ is the azimuthal angle between $\mathbf{k}_{1,t}$ and $\mathbf{k}_{2,t}$. In our case, in contrast to vector-vector fusion to pseudoscalars, $\phi \neq \Phi$. This may cause a deviation from $\sin^2(\Phi)$ distribution. To better illustrate the deviation we write the gluon-gluon-pseudoscalar meson coupling in the following equivalent way

$$V(k_1, k_2, P_M) = -V_N\frac{s}{2}F_{g^*g^*\to\eta'}(k_{1,t}^2, k_{2,t}^2) \times [|\mathbf{p}'_{1,t}||\mathbf{p}'_{2,t}|\sin(\Phi) - |\mathbf{k}_{0,t}||\mathbf{p}'_{1,t}| \times \sin(\psi + \Phi) + |\mathbf{k}_{0,t}||\mathbf{p}'_{2,t}|\sin(\psi)]. \quad (2.11)$$

Here Φ is explicitly the azimuthal angle between the transverse momenta of outgoing protons $\mathbf{p}'_{1,t}$ and $\mathbf{p}'_{2,t}$, ψ is the azimuthal angle between $\mathbf{k}_{0,t}$ and $\mathbf{p}'_{2,t}$ $(0 < \psi < 2\pi)$.

It is convenient to introduce the dimensionless parameters

$$\mu = \frac{|\mathbf{k}_{0,t}|}{m_{\eta'}}, \qquad \xi = \frac{|\mathbf{p}'_{1,t}|}{m_{\eta'}}, \qquad \eta = \frac{|\mathbf{p}'_{2,t}|}{m_{\eta'}}.$$

We take $k_{0,t}^2 = -|\mathbf{k}_{0,t}|^2$, $k_{1,t}^2 = -|\mathbf{k}_{1,t}|^2$, $k_{2,t}^2 = -|\mathbf{k}_{2,t}|^2$ and write differential $d^2k_{0,t}$ as: $d^2k_{0,t} = -|\mathbf{k}_{0,t}|d|\mathbf{k}_{0,t}|d\psi$. Then we obtain finally

$$\mathcal{M}^{g^*g^*\to\eta'}_{pp\to p\eta' p}(\xi, \eta, \Phi, m_{\eta'}) = -V_N i\pi^2\frac{s}{2m_{\eta'}^2}\int\frac{d\mu}{\mu}\int_0^{2\pi}d\psi\frac{[\xi\eta\sin(\Phi) - \mu\xi\sin(\psi + \Phi) + \mu\eta\sin(\psi)]}{[\mu^2 + \xi^2 + 2\mu\xi\cos(\psi + \Phi)][\mu^2 + \eta^2 - 2\mu\eta\cos(\psi)]} \times f^{\text{off}}_{g,1}(x_1, x'_1, k_{0,t}^2, k_{1,t}^2, t_1)f^{\text{off}}_{g,2}(x_2, x'_2, k_{0,t}^2, k_{2,t}^2, t_2)F_{g^*g^*\to\eta'}(k_{1,t}^2, k_{2,t}^2). \quad (2.12)$$

We have to take into account that the dimensionless arguments in $f^{\text{off}}_{g,1}$, $f^{\text{off}}_{g,2}$ and $F_{g^*g^*\to\eta'}$

$$\frac{k_{0,t}^2}{m_{\eta'}^2} = -\mu^2,$$
$$\frac{k_{1,t}^2}{m_{\eta'}^2} = -\mu^2 - \xi^2 - 2\mu\xi\cos(\psi + \Phi),$$
$$\frac{k_{2,t}^2}{m_{\eta'}^2} = -\mu^2 - \eta^2 + 2\mu\eta\cos(\psi)$$

are the functions of integration variables μ and ψ. So now we clearly see there is no simple angular behavior like $\mathcal{M} \sim \sin(\Phi)$. The angular behavior of matrix element is more complicated. Only in the limit $k_{0,t} \to 0$ the $\sin(\Phi)$-behavior with some modulated amplitude is restored.

We can obtain some information about angular behavior of matrix element from properties of the integral (2.12). Obviously, we have periodicity of $\mathcal{M}$ in Φ with the period 2π. For $\Phi = 0$ and $\Phi = \pi$ we have immediately $\mathcal{M} = 0$. It follows from the oddness of the integrand for these values of Φ. This investigation is a good check of numerical results shown at Fig. (10). Of course, more detailed

information can be obtained only after numerical integration of (2.12) with concrete functions $f_{g,1}^{\rm off}$, $f_{g,2}^{\rm off}$ and $F_{g^*g^*\to\eta'}$.

The objects $f_{g,1}^{\rm off}(x_1, x_1', k_{0,t}^2, k_{1,t}^2, t_1)$ and $f_{g,2}^{\rm off}(x_2, x_2', k_{0,t}^2, k_{2,t}^2, t_2)$ appearing in formula (2.4) and (2.12) are skewed (or off-diagonal) unintegrated gluon distributions. They are nondiagonal both in x and k_t^2 space. Usual off-diagonal gluon distributions are nondiagonal only in x. In the limit $x_{1,2} \to x_{1,2}'$, $k_{0,t}^2 \to k_{1/2,t}^2$ and $t_{1,2} \to 0$ they become usual UGDFs.

Using the relations (2.1) and $k_1 - k_2 = P_M$ and $s \gg |\mathbf{k}_{0,t}|^2$, we obtain

$$\begin{aligned} s x_1 x_2 &= m_{\eta'}^2 + |\mathbf{p}_{1,t}'|^2 + |\mathbf{p}_{2,t}'|^2 + 2|\mathbf{p}_{1,t}'||\mathbf{p}_{2,t}'|\cos(\Phi) \\ &= m_{\eta'}^2 + |\mathbf{P}_{M,t}|^2. \end{aligned} \tag{2.13}$$

The longitudinal momentum fractions are now calculated as:

$$x_{1,2} = \frac{m_{\eta'}^2 + |\mathbf{P}_{M,t}|^2}{s}\exp(\pm y), \qquad x_{1,2}' = x_0 = \frac{|\mathbf{k}_{0,t}|}{\sqrt{s}}. \tag{2.14}$$

Above y is the rapidity of the produced meson.

In the general case we do not know UGDFs very well. It seems reasonable, at least in the first approximation, to take

$$f_{g,1}^{\rm off}(x_1, x_1', k_{0,t}^2, k_{1,t}^2, t_1) = \sqrt{f_g^{(1)}(x_1', k_{0,t}^2)\cdot f_g^{(1)}(x_1, k_{1,t}^2)}\cdot F_1(t_1), \tag{2.15}$$

$$f_{g,2}^{\rm off}(x_2, x_2', k_{0,t}^2, k_{2,t}^2, t_2) = \sqrt{f_g^{(2)}(x_2', k_{0,t}^2)\cdot f_g^{(2)}(x_2, k_{2,t}^2)}\cdot F_1(t_2), \tag{2.16}$$

where $F_1(t_1)$ and $F_1(t_2)$ are usual Dirac isoscalar nucleon form factors and t_1 and t_2 are total four-momentum transfers in the first and second proton line, respectively. The above prescription is a bit arbitrary, although it is inspired by the positivity constraints [16] for *collinear* Generalized Parton Distributions. It provides, however, an interpolation between different x and k_t values appearing kinematically. Our prescription is more symmetric in variables of the first and second exchange than the one used recently in [17] for Higgs boson production.

The UGDFs above have a property that

$$f(x, k_t^2) \to 0, \tag{2.17}$$

if $k_t^2 \to 0$. The small-k_t^2 region is of nonperturbative nature and is rather modeled than derived from pQCD. Usually the UGDFs in the literature are modeled to fulfill

$$\frac{f(x, k_t^2)}{k_t^2} = \mathcal{F}(x, k_t^2) \to \text{const} \tag{2.18}$$

if $k_t^2 \to 0$. It is sometimes more useful to use $\mathcal{F}(x, k_t^2)$ instead of $f(x, k_t^2)$.

When inspecting Eq. (2.4) and (2.16) it becomes clear that the cross section for elastic double-diffractive production of a meson (or Higgs boson) is much more sensitive to the choice of UGDFs than the inclusive cross sections.

B. $\gamma^*\gamma^*$ fusion

It was advocated in Ref. [18] that the pseudoscalar mesons production at small transverse momenta may be dominated by the virtual photon—virtual photon fusion. In the following we wish to investigate the competition of the diffractive mechanism discussed in the previous subsection and the $\gamma^*\gamma^*$ fusion mechanism.

In this case averaged matrix element squared

$$\overline{|\mathcal{M}|^2} = \frac{1}{4}\sum |\mathcal{M}_{\lambda_1,\lambda_2,\lambda_1',\lambda_2'}|^2. \tag{2.19}$$

In the most general case the Born amplitude (for notation see Fig. 4) reads:

$$\begin{aligned} \mathcal{M}_{\lambda_1,\lambda_2,\lambda_1',\lambda_2'} = &\left\{\overline{u}(p_1', \lambda_1')\left[F_1(t_1)\gamma^\mu \pm i\frac{\sigma^{\mu\mu''}}{2M_N}k_{1,\mu''}F_2(t_1)\right]u(p_1, \lambda_1)\right\}\frac{g_{\mu\mu'}}{t_1}(-i)e^2 F_{\gamma^*\gamma^*\to\eta'}(t_1, t_2)\epsilon_{\mu'\nu'\alpha,\beta}k_1^\alpha k_2^\beta\frac{g_{\nu\nu'}}{t_2} \\ &\times\left\{\overline{u}(p_2', \lambda_2')\left[F_1(t_2)\gamma^\nu \pm i\frac{\sigma^{\nu\nu''}}{2M_N}k_{1,\nu''}F_2(t_2)\right]u(p_2, \lambda_2)\right\}. \end{aligned} \tag{2.20}$$

Limiting to large energies ($\sqrt{s} \gg m_{\eta'} + M_N + M_N$) and small transverse momenta t_1 and t_2 ($|t| \ll 4M_N^2$) the matrix element for $pp \to p\eta' p$ reaction via virtual photon—virtual photon fusion can be written as

$$\begin{aligned} \mathcal{M}_{pp\to p\eta' p}^{\gamma^*\gamma^*\to\eta'} \approx &\, eF_1(t_1)\frac{(p_1 + p_1')^\mu}{t_1}\Gamma_{\mu\nu}^{\gamma^*\gamma^*\to\eta'}(k_1, k_2) \\ &\times\frac{(p_2 + p_2')^\nu}{t_2}eF_1(t_2), \end{aligned} \tag{2.21}$$

where

$$\Gamma_{\mu\nu}^{\gamma^*\gamma^*\to\eta'}(k_1, k_2) = -ie^2 F_{\gamma^*\gamma^*\to\eta'}(k_1^2, k_2^2)\epsilon_{\mu\nu\rho\sigma}k_1^\rho k_2^\sigma. \tag{2.22}$$

In Eq. (2.21) $F_1(t_1)$ and $F_1(t_2)$ are Dirac proton electromagnetic form factors. In the following we have omitted the spin-flipping contributions related to the respective Pauli form factors. $F_{\gamma^*\gamma^*\to\eta'}$ is a respective electromagnetic off-shell form factor normalized to

$$F_{\gamma^*\gamma^*\to\eta'}(0,0) = \frac{1}{4\pi^2 f_{\eta'}}, \tag{2.23}$$

where $f_{\eta'}$ is the meson decay constant. Alternatively one can use the relation

$$|F_{\gamma^*\gamma^*\to\eta'}(0,0)|^2 = \frac{1}{(4\pi\alpha)^2}\frac{64\pi\Gamma(\eta'\to\gamma\gamma)}{m_{\eta'}^3}, \tag{2.24}$$

where only measured quantities enter. Inserting PDG values of experimental entries for η' we get $|F_{\gamma^*\gamma^*\to\eta'}(0,0)|^2 = 0.116\ \mathrm{GeV}^{-2}$.

Now we can write

$$(p_1 + p_1')^\mu \Gamma^{\gamma^*\gamma^*\to\eta'}_{\mu\nu}(k_1,k_2)(p_2+p_2')^\nu \approx -ie^2\cdot(2s)F_{\gamma^*\gamma^*\to\eta'}(k_1^2,k_2^2)|\mathbf{k}_{1,t}||\mathbf{k}_{2,t}|\sin(\Phi). \tag{2.25}$$

Collecting all ingredients together we get

$$\overline{|\mathcal{M}^{\gamma^*\gamma^*\to\eta'}_{pp\to p\eta' p}|^2} \approx 4s^2e^8\frac{F_1^2(t_1)}{t_1^2}\frac{F_1^2(t_2)}{t_2^2}|F_{\gamma^*\gamma^*\to\eta'}(k_1^2,k_2^2)|^2 \times |\mathbf{k}_{1,t}|^2|\mathbf{k}_{2,t}|^2\sin^2(\Phi). \tag{2.26}$$

The t_1 and t_2 dependences of $F_{\gamma^*\gamma^*\to\eta'}$ are the least known ingredients in the formula (2.26). It is known experimentally only for one virtual photon. In the following we shall use two different forms of the form factors. The first one is inspired by the vector-dominance model:

$$F_{\gamma^*\gamma^*\to\eta'}(k_1^2,k_2^2) = \frac{F_{\gamma^*\gamma^*\to\eta'}(0,0)}{(1-k_1^2/m_\rho^2)(1-k_2^2/m_\rho^2)}. \tag{2.27}$$

The second one is motivated by the leading twist pQCD analysis in Ref. [19]:

$$F_{\gamma^*\gamma^*\to\eta'}(k_1^2,k_2^2) = \frac{F_{\gamma^*\gamma^*\to\eta'}(0,0)}{(1-(k_1^2+k_2^2)/m_\rho^2)}. \tag{2.28}$$

Both these forms describe the CLEO data [20] for one real and one virtual photon.

C. Phase space and kinematics

The cross section for the 3-body reaction $pp \to p\eta' p$ can be written as

$$d\sigma = \frac{1}{2s}\overline{|\mathcal{M}|^2}\cdot d^3PS. \tag{2.29}$$

The three-body phase-space volume element reads

$$d^3PS = \frac{d^3p_1'}{2E_1'(2\pi)^3}\frac{d^3p_2'}{2E_2'(2\pi)^3}\frac{d^3P_M}{2E_M(2\pi)^3}\cdot(2\pi)^4\delta^4(p_1+p_2-p_1'-p_2'-P_M). \tag{2.30}$$

At high energies and small momentum transfers the phase-space volume element can be written as

$$d^3PS = \frac{1}{2^8\pi^4}dt_1dt_2d\xi_1d\xi_2d\Phi\,\delta(s(1-\xi_1)(1-\xi_2)-m_{\eta'}^2), \tag{2.31}$$

where ξ_1, ξ_2 are longitudinal momentum fractions carried by outgoing protons with respect to their parent protons and the relative angle between outgoing protons $\Phi \in (0, 2\pi)$. Changing variables $(\xi_1, \xi_2) \to (x_F, m_{\eta'}^2)$ one gets

$$d^3PS = \frac{1}{2^8\pi^4}dt_1dt_2\frac{dx_F}{s\sqrt{x_F^2+4(m_{\eta'}^2+|\mathbf{P}_{M,t}|^2)/s}}d\Phi. \tag{2.32}$$

It is more convenient for lower (but still high) energy to use variable x_F. However, at very high energies the cross section becomes too much peaked at $x_F \approx 0$ due to the jacobian

$$J \approx \frac{1}{\sqrt{x_F^2+4m_{\eta'}^2/s}} \to \frac{\sqrt{s}}{2m_{\eta'}} \tag{2.33}$$

and the use of rapidity y instead of x_F is recommended. The phase-space element in this case has the following simple form

$$d^3PS = \frac{1}{2^8\pi^4 s}dt_1dt_2dyd\Phi. \tag{2.34}$$

If x_F is used then

$$\xi_{1,2} \approx 1 - \frac{1}{2}\sqrt{x_F^2+\frac{4m_{\eta'}^2}{s}} \mp \frac{x_F}{2}. \tag{2.35}$$

In the other case when the meson rapidity is used then

$$\xi_{1,2} \approx 1 - \frac{m_{\eta'}}{\sqrt{s}}\exp(\pm y). \tag{2.36}$$

Now the four-momentum transfers in both proton lines can be calculated as

$$t_{1,2} = -\frac{p_{1/2,t}'^2}{\xi_{1,2}} - \frac{(1-\xi_{1,2})^2m_p^2}{\xi_{1,2}}. \tag{2.37}$$

Only if $\xi_{1,2} = 1$, $t_{1,2} = -p_{1/2,t}'^2$. The latter approximate relation was often used in earlier works on diffractive production of particles. However, in practice $\xi_{1,2} \neq 0$ and the more exact equation must be used. The range of t_1 and t_2 is not unlimited as it is often assumed. One can read off from Eq. (2.37) a kinematical upper limit for $t_{1,2}$ which is:

$$t_{1,2} < -\frac{(1-\xi_{1,2})^2}{\xi_{1,2}}m_p^2. \tag{2.38}$$

In practice these phase-space limits become active only for $|x_F| > 0.2$. The lower limits are energy dependent but are not active in practice.

The Mandelstam variables for subsystems $\{\text{proton}_1' + \eta'\}$ and $\{\text{proton}_2' + \eta'\}$ can be expressed via other kinematical variables

$$s_{1,2} = s(1 - \xi_{1,2}) + m_p^2 + 2t_{1,2}. \tag{2.39}$$

It is also checked if $s_{1,2} > (m_{\eta'} + m_p)^2$, but this limit is not active in the region of interest (central production).

III. RESULTS

Before we present our results let us discuss some input parameters for our calculations.

The partial decay width $\Gamma(\eta' \to gg)$ is not well known. Of course

$$\Gamma(\eta' \to gg) < \Gamma^{\text{tot}}_{\eta'} \approx 0.2 \text{ MeV}. \tag{3.1}$$

In the following we shall take the upper limit in order to estimate the cross section.

The form factors responsible for off-diagonal effects are taken in the form [21]

$$F_1(t_{1,2}) = \frac{4m_p^2 - 2.79t_{1,2}}{(4m_p^2 - t_{1,2})(1 - t_{1,2}/071)^2}. \tag{3.2}$$

The proton form factor in this form gives rather good description of the t-dependence of the elastic pp cross section at high energies, i.e. for kinematics similar as in our case.

The k_1^2 and k_2^2 dependence of the form factor $F_{g^*g^* \to \eta'}(k_1^2, k_2^2)$ is not well known as it is due to nonperturbative effects related to the internal structure of the η'-meson. In the following, in analogy to the $\gamma^*\gamma^* \to \eta'$ form factor, we take it in the factorized double monopole form

$$F_{g^*g^* \to \eta'}(k_1^2, k_2^2) = \frac{1}{(1 - k_1^2/\Lambda_{os}^2)(1 - k_2^2/\Lambda_{os}^2)}. \tag{3.3}$$

We take $k_1^2 = -k_{1,t}^2$ and $k_2^2 = -k_{2,t}^2$. The parameter $\Lambda_{os} \sim m_\rho$ may be expected. In general, it can be treated as a free parameter in order to quantify the theoretical uncertainties.

In the present work we shall use a few sets of unintegrated gluon distributions which aim at the description of phenomena where small gluon transverse momenta are involved. Some details concerning the distributions can be found in Ref. [22]. We shall follow the notation there.

The larger energies, the smaller values of parton momentum fractions come into game. Therefore at larger energies we shall use distributions constructed exclusively for small values of x. Two of them are based on the idea of gluon saturation. One of them was obtained based on a saturation-inspired parametrization of the dipole-nucleon cross section which leads to a good description of the HERA data [23]. The second one [24] was constructed to describe the inclusive RHIC pion spectra. The third one is the asymptotic BFKL distribution [25]. We do not wish to repeat more details here. It can be found in individual references as well as in Ref. [22] where applications of UGDFs to $c\bar{c}$ correlations was discussed.

Because of its simplicity the Gaussian smearing of initial transverse momenta is a good reference point for other approaches. It allows to study phenomenologically the role of transverse momenta in several high-energy processes. We define simple unintegrated gluon distribution:

$$\mathcal{F}_g^{\text{Gauss}}(x, k_t^2, \mu_F^2) = xg^{\text{coll}}(x, \mu_F^2) \cdot f_{\text{Gauss}}(k_t^2), \tag{3.4}$$

where $g^{\text{coll}}(x, \mu_F^2)$ are standard collinear (integrated) gluon distribution and $f_{\text{Gauss}}(k_t^2)$ is a Gaussian two-dimensional function:

$$f_{\text{Gauss}}(k_t^2) = \frac{1}{2\pi\sigma_0^2} \exp(-k_t^2/2\sigma_0^2)/\pi. \tag{3.5}$$

The UGDF defined by Eq. (3.4) and (3.5) are normalized such that:

$$\int \mathcal{F}_g^{\text{Gauss}}(x, k_t^2, \mu_F^2) dk_t^2 = xg^{\text{coll}}(x, \mu_F^2). \tag{3.6}$$

In the present paper we shall not use Khoze-Martin-Ryskin UGDFs. The main reason is that in our case the KMR prescription can be used only in a very limited range of gluon transverse momenta $Q_0^2 < k_t^2 < m_{\eta'}^2$, where Q_0^2 is the lowest possible perturbative scale. In the case of light meson production we are sensitive mainly to the nonperturbative region $k_t < Q_0$ where KMR method cannot be directly applied. Its application would require unclear extrapolation to the other regions. We feel this is a quite arbitrary procedure.

Furthermore KMR uses some approximation when deriving off-diagonal UGDFs assuming $k_{0,t} \gg p_{1,t}', p_{2,t}'$. We have checked that in our case this in not a good approximation. In Fig. 5 we show results with and without this

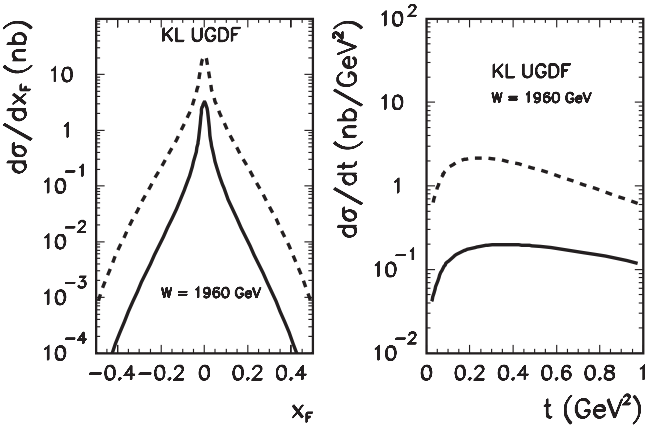

FIG. 5. Cross sections for different prescriptions for off-diagonal UGDFs. The solid line corresponds to our prescription and the dashed line corresponds to the KMR prescription $k_{1t} = k_{2t} = k_{0t}$. In this calculation we have taken KL distribution. No absorption corrections were included here.

approximation applied to the off-diagonal UGDFs. These results differ significantly.

In our case, unlike for the Higgs production, we are extremely sensitive to small transverse momenta of the order of a fraction of GeV, i.e. to a nonperturbative region. However, some UGDFs like KL were constructed for this nonperturbative region so we think their use is justified. In Fig. 6 we show results for different lower cuts on gluon transverse momenta. This result clearly shows the role of small gluon transverse momenta.

We wish to stress in this context that all the distributions considered give quite reasonable description of the HERA F_2 data. It was discussed by one of the authors that HERA data does not provide strong contraints on k_t-dependence of UGDFs. Different UGDFs lead to different predictions for other inclusive reactions [22,26]. Similar observation was made by Lonnblad and Sjödahl for exclusive Higgs production [27].

The two-scale off-diagonal distributions require a separate discussion. In this case

$$f_{g,1}^{\rm off} = \sqrt{f_g^{(1)}(x_1', k_{0,t}^2, \mu_0^2) \cdot f_g^{(1)}(x_1, k_{1,t}^2, \mu^2)} \cdot F_1(t_1), \quad (3.7)$$

$$f_{g,2}^{\rm off} = \sqrt{f_g^{(2)}(x_2', k_{0,t}^2, \mu_0^2) \cdot f_g^{(2)}(x_2, k_{2,t}^2, \mu^2)} \cdot F_1(t_2), \quad (3.8)$$

The choice of the (factorization) scales here is not completely obvious. We shall try the following six choices:

$$(a1)\ \mu_0^2 = m_{\eta'}, \qquad \mu^2 = m_{\eta'}^2,$$
$$(a2)\ \mu_0^2 = m_{\eta'}, \qquad \mu^2 = m_{\eta'}^2 + P_{M,t}^2,$$
$$(b1)\ \mu_0^2 = Q_0^2, \qquad \mu^2 = m_{\eta'}^2,$$
$$(b2)\ \mu_0^2 = Q_0^2, \qquad \mu^2 = m_{\eta'}^2 + P_{M,t}^2,$$
$$(c1)\ \mu_0^2 = k_{0,t}^2 (+\text{freezing at } k_{0,t}^2 < Q_0^2), \qquad \mu^2 = m_{\eta'}^2,$$
$$(c2)\ \mu_0^2 = k_{0,t}^2 (+\text{freezing at } k_{0,t}^2 < Q_0^2), \quad \mu^2 = m_{\eta'}^2 + P_{M,t}^2.$$

The first choice is similar as in [28]. However, it is not obvious if the scale associated with the "hard" production ($g^*g^* \to \eta'$) can be used for the left part of the gluonic ladder where no obvious hard scale appears. Therefore we shall try also the second choice where we shall use $Q_0^2 = 0.26$ GeV^2, i.e. the nonperturbative input for the QCD evolution in Ref. [29]. Another option was proposed by Lonnblad and Sjödahl [27]. They take $k_{0,t}^2$ as a first scale. In our case this prescription must be supplemented by freezing the scale for gluon transverse momenta smaller than Q_0 (minimal perturbative scale). Since η' mass is rather small we shall try also transverse mass $\mu^2 = m_{\eta'}^2 + P_{M,t}^2$ for the second scale. In Fig. 7 we show $d\sigma/dx_F$ and $d\sigma/dt_{1,2}$ for different choices of both scales. We observe a strong dependence on the choice of the first (μ_0^2) scale. The adding transverse momentum of the η' meson in (a2), (b2) and (c2) (dashed lines in the figures) change the results insignificantly.

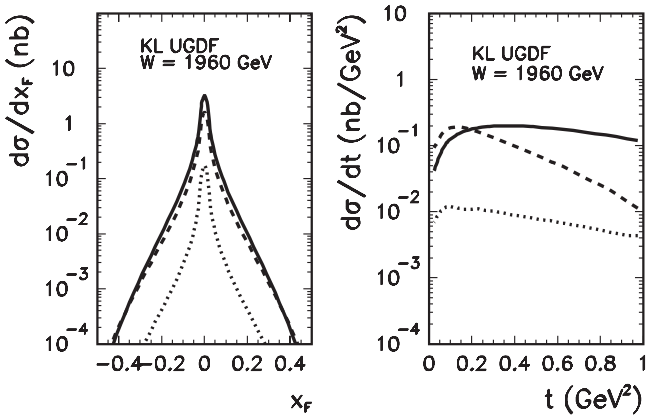

FIG. 6. Dependence of the cross section on the lower cut on gluon transverse momenta. Solid line corresponds to no cut case, dashed line to $k_{t,\min}^2 = 0.2$ GeV^2 and the dotted line to $k_{t,\min}^2 = 0.4$ GeV^2. No absorption correctons were included here.

Now we shall present results for various UGDFs. Let us start from the $d\sigma/dx_F$ distribution. In Fig. 8 we show the results of calculations obtained with several models of UGDF (for details see [22]). For comparison we show also the contribution of the $\gamma^*\gamma^*$ fusion mechanism. The contribution of the last mechanism is much smaller than the contribution of the diffractive QCD mechanism.

In Fig. 9 we present distribution in t_1 and t_2 (identical) of the diffractive production and of the $\gamma^*\gamma^*$ mechanism (red dash-dotted curve). The distribution for the $\gamma^*\gamma^*$ fusion is much steeper than that for the diffractive production.

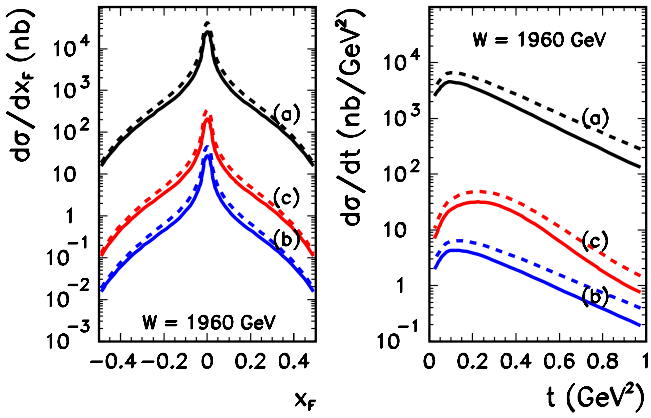

FIG. 7 (color online). Dependence of the cross section on factorization scales for the Gaussian off-diagonal UGDFs. The solid lines correspond to $\mu^2 = m_{\eta'}^2$ and the dashed lines correspond $\mu^2 = m_{\eta'}^2 + P_{M,t}^2$. Three pairs of lines correspond to different choices of $\mu_0^2 = m_{\eta'}^2$ (a), k_{0t}^2(+freezing) (c), Q_0^2 (b) (from top to bottom). No absorption corrections were included here.

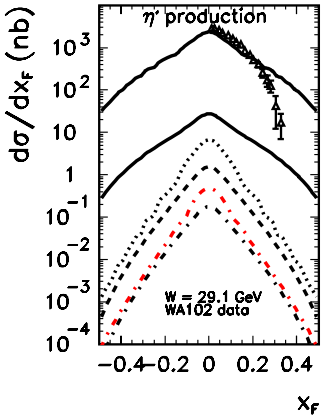

FIG. 8 (color online). $d\sigma/dx_F$ as a function of Feynman x_F for $W = 29.1$ GeV and for different UGDFs. The $\gamma^*\gamma^*$ fusion contribution is shown by the dash-dotted (red) line (second from the bottom). The experimental data of the WA102 collaboration [12] are shown for comparison. The dashed line corresponds to the KL distribution, dotted line to the GBW distribution and the dash-dotted to the BFKL distribution. The two solid lines correspond to the Gaussian distribution with (a1) (upper) and (b1) (lower) choices of scales. No absorption corrections were included here.

In Fig. 10 we show the distribution of the cross section as a function of the angle between the outgoing protons. In the first approximation it reminds $\sin^2(\Phi)$. A more detailed inspection shows, however, that the distribution is somewhat skewed with respect to $\sin^2(\Phi)$ dependence. This is due to the two reasons:

(a) kinematical—caused by interrelations of integration variables due to finite phase-space limits (present also for the pomeron + pomeron $\rightarrow \eta'$ fusion model),

(b) dynamical—caused by nonlocality due to the inter-

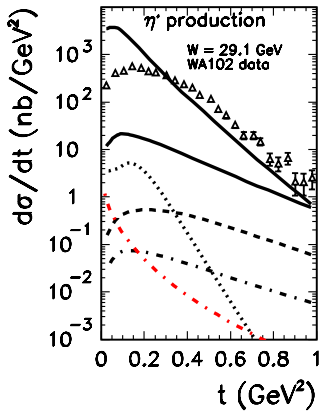

FIG. 9 (color online). $d\sigma/dt_{1/2}$ as a function of Feynman $t_{1/2}$ for $W = 29.1$ GeV and for different UGDFs. The $\gamma^*\gamma^*$ fusion contribution is shown by the dash-dotted (red) steeply falling down line. The experimental data of the WA102 collaboration [12] are shown for comparison. The notation here is the same as in Fig. 8. No absorption corrections were included here.

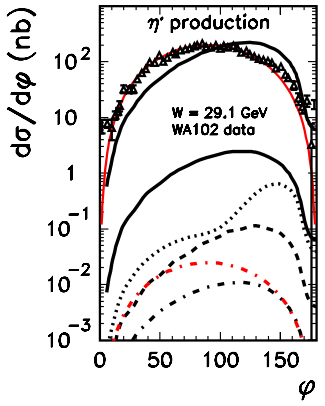

FIG. 10 (color online). $d\sigma/d\Phi$ as a function of Φ for $W = 29.1$ GeV and for different UGDFs. The $\gamma^*\gamma^*$ fusion contribution is shown by the dash-dotted (red) symmetric around 90° line. The experimental data of the WA102 collaboration [12] are shown for comparison. The notation here is the same as in Fig. 8. No absorption corrections were included here.

nal loop of the diagram shown in Fig. 1 (the $\sin(\phi)$ dependence is embedded only in the loop integration).

In order to quantify the effect we define the parameter of the skewedness of the Φ distribution as

$$S_{\pi/2}(W) \equiv \frac{\int_{\pi/2}^{\pi} \frac{d\sigma}{d\Phi}(W)d\Phi - \int_{0}^{\pi/2} \frac{d\sigma}{d\Phi}(W)d\Phi}{\int_{0}^{\pi} \frac{d\sigma}{d\Phi}(W)d\Phi}. \quad (3.9)$$

If we take more differential cross section in the definition above than $S_{\pi/2} = S_{\pi/2}(W, y, t_1, t_2)$ (or $S_{\pi/2}(W, x_F, t_1, t_2)$). Of course $-1 < S_{\pi/2} < 1$. For exact $\sin^2(\Phi)$ distribution $S_{\pi/2} = 0$. In Table I we show the skewedness parameter $S_{\pi/2}$ for our model for different initial energies $W = 29.1$, 200, 1960, 14000 GeV, relevant for WA102, RHIC, Tevatron and LHC, respectively. Generally, the larger energies the smaller $S_{\pi/2}$. The phase-space limitations cause only a very small skewedness.

In Table II and in Fig. 11 we show energy dependence of the total (integrated over kinematical variables) cross section for the exclusive reaction $pp \rightarrow p\eta' p$ for different UGDFs. In the case of Gaussian UGDFs we show in

TABLE I. The measure of the skewedness $S_{\pi/2}$ of azimuthal angle distributions for different UGDFs and different center-of-mass energies. In this calculation $-0.5 < x_F < 0.5$, -1 GeV $< t_{1,2} < 0$.

W (GeV)	$S_{\pi/2}$ (KL)	$S_{\pi/2}$ (GBW)	$S_{\pi/2}$ (BFKL)
29.1	0.5990	0.7889	0.3615
200	0.5867	0.6628	0.3131
500	0.5629	0.4983	0.2990
1960	0.5019	0.2622	0.2814
14000	0.3870	0.2283	0.2617

TABLE II. Energy dependence of the cross section (in nb) for different UGDFs. The integration is over $-4 < y < 4$ and -1 GeV $< t_{1,2} < 0$. The second lines for Gaussian distributions are for the choice (b) of the factorization scale. No absorption corrections were included.

UGDF	29.1	200	1960
KL	0.2867(+0)	0.7377(+0)	0.4858(+0)
GBW	0.1106(+1)	0.2331(+2)	0.1034(+3)
BFKL	0.3279(−1)	0.9205(+1)	0.2188(+4)
Gauss (0.2)	0.6391(+3)	0.1697(+5)	0.2964(+6)
	0.3445(+1)		0.2984(+3)
Gauss (0.5)	0.7389(+1)	0.2705(+3)	0.3793(+3)
	0.4199(−1)		0.4094(+1)
$\gamma^*\gamma^*$	0.7764(−1)	0.2260(+0)	0.3095(+0)

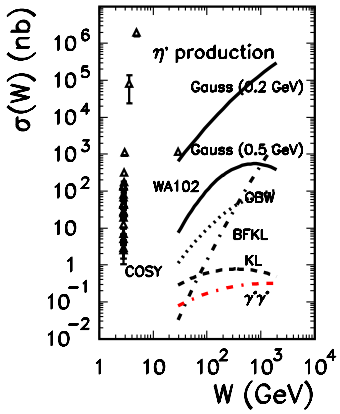

FIG. 11 (color online). $\sigma_{\rm tot}$ as a function of center-of-mass energy for different UGDFs. The $\gamma^*\gamma^*$ fusion contribution is shown by the dash-dotted (red) line. The world experimental data are shown for reference. The notation here is the same as in Fig. 8. No absorption corrections were included here.

Table II also results with the second choice of the factorization scale. The cross section with the second choice is much smaller than the cross section with the first choice. Quite different results are obtained for different UGDFs. This demonstrates once again the huge sensitivity to the choice of UGDF. The cross section with the Kharzeev-Levin type distribution (based on the idea of gluon saturation) gives the cross section which is small and almost idependent of beam energy. In contrast, the BFKL distribution leads to strong energy dependence. The sensitivity to the transverse momenta of initial gluons can be seen by comparison of the two solid lines calculated with the Gaussian UGDF with different smearing parameter $\sigma_0 =$ 0.2 and 0.5 GeV. The contribution of the $\gamma^*\gamma^*$ fusion mechanism (red dash-dotted line) is fairly small and only slowly energy dependent. While the QED contribution can be reliably calculated, the QCD contribution cannot be at present fully controlled. It is even not completely excluded that the QED contribution dominates over the QCD contribution in some energy window.

At present it seems impossible to understand the dynamics of the exclusive η' production at high energy without a real measurement. The Tevatron apparatus gives such a possibility, at least in principle. In Fig. 12 we present two-dimensional maps $t_1 \times t_2$ of the cross section for the QCD mechanism (KL UGDF) and the QED mechanism (Dirac terms only) for the Tevatron energy $W = 1960$ GeV. If $|t_1|, |t_2| > 0.5$ GeV^2 the QED mechanism is clearly negligible. However, at $|t_1|\ |t_2| < 0.2$ GeV^2 the QED mechanism may become equally important or even dominant. In addition, it may interfere with the QCD mechanism.

In Fig. 13 we show a two-dimensional map $t \times \Phi$, where $t = t_1$ or t_2. The bigger t, the larger skewedness with respect to $\Phi = \pi/2$. The skewedness, which is almost independent of the beam energy, is a generic feature of the QCD mechanism, quite independent of the choice of UGDF. The observation of the skewedness seems to be a

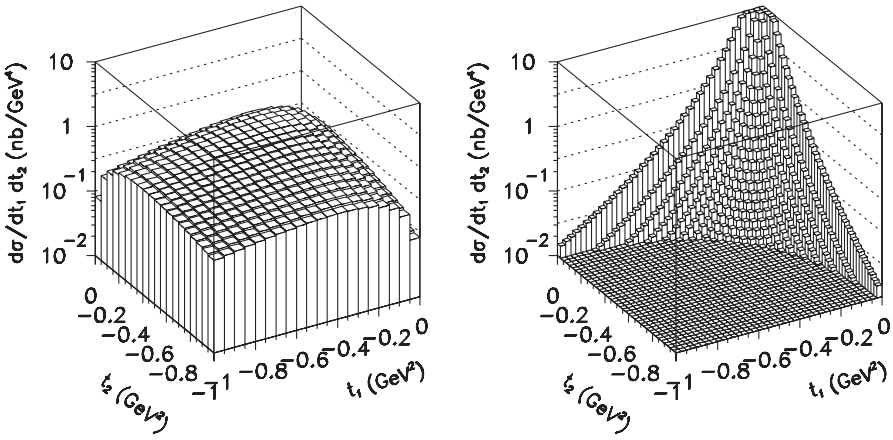

FIG. 12. Two-dimensional distribution in $t_1 \times t_2$ for the diffractive QCD mechanism (left panel), calculated with the KL UGDF, and the $\gamma^*\gamma^*$ fusion (right panel) at the Tevatron energy $W = 1960$ GeV. No absorption corrections were included here.

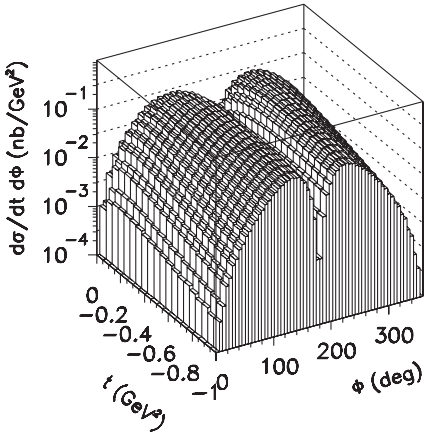

FIG. 13. The cross section for $p\bar{p} \to p\eta'\bar{p}$ as a function of t (t_1 or t_2) and relative azimuthal angle Φ for the Tevatron energy $W = 1960$ GeV. In this calculation the KL UGDF was used. No absorption corrections were included here.

condition ''sine qua non'' for the confirmation of the QCD mechanism.[3] On the other hand, the observation of the $\sin^2\Phi$ dependence, as for the lower-energy WA102 data, may be very difficult to understand microscopically.

Summarizing, the reaction under consideration seems very promissing in better understanding of the QCD dynamics in the nonperturbative region.

In the case of Higgs (or heavy particle) production the large mass sets a hard scale. In the case of η' the mass is only about 1 GeV. In this case the hard scale can be obtained by selecting large transverse momenta or analogously large $|t_1|$ and $|t_2|$. In principle, these variables could be controlled by measuring outgoing protons. As an example in Table III we have collected results for different windows in the (t_1, t_2) space for the KL UGDF. In this case the cross section is dropping down rather slowly with increasing $|t_1|$ and $|t_2|$. However, this result depends strongly on UGDF used in the calculation. Therefore measuring the cross section for different cuts on t_1 and t_2 would be a farther test of UGDFs.

The formalism presented in the previous sections can be applied to a production of other pseudoscalar mesons. In Table IV we have collected cross sections for η_c meson integrated over broad range of kinematical variables specified in the table caption. Again we have taken an upper limit assuming $\Gamma(\eta_c \to gg) = \Gamma^{\rm tot}_{\eta_c}$, which may be even more reliable in the case of η_c production. These cross sections are very similar to the cross section for η' production and in some cases even bigger. The results with Gaussian distribution, $\sigma_0 = 0.2$ GeV and first choice of factorization scale seems excluded, as constituting too large fraction of the total cross section. This strongly suggests also that the analogous result for η' production must be questioned. This seems to open a problem of understanding the WA102 data in terms of the QCD mechanism discussed above.

[3]The absorption corrections should only increase the skewedness.

TABLE III. Cross section in nb for different cuts on t_1 and t_2 and $-0.5 < x_F < 0.5$. The limits for the $(-t_1)$ and $(-t_2)$ windows in GeV^2 are given explicitly. This calculation was done for the KL UGDF. No absorption corrections were included.

	(0,1)	(1,2)	(2,3)	(3,4)
(0,1)	0.1587(0)	0.5437(−1)	0.8436(−2)	0.1558(−2)
(1,2)	0.5437(−1)	0.2257(−1)	0.4033(−2)	0.7978(−3)
(2,3)	0.8436(−2)	0.4033(−2)	0.9033(−3)	0.2089(−3)
(3,4)	0.1558(−2)	0.7978(−3)	0.2089(−3)	0.5753(−4)

TABLE IV. Comparison of the cross section (in nb) for η' and η_c production at Tevatron ($W = 1960$ GeV) for different UGDFs. The integration is over $-4 < y < 4$ and -1 GeV $< t_{1,2} < 0$. The second lines for Gaussian distributions are for the choice (a2) of the factorization scale. No absorption corrections were included.

UGDF	η'	η_c
KL	0.4858(+0)	0.7392(+0)
GBW	0.1034(+3)	0.2039(+3)
BFKL	0.2188(+4)	0.1618(+4)
Gauss (0.2)	0.2964(+6)	0.3519(+8)
	0.2984(+3)	0.2104(+4)
Gauss (0.5)	0.3793(+3)	0.4417(+6)
	0.4094(+1)	0.3008(+2)
$\gamma^*\gamma^*$	0.3095(+0)	0.4493(+0)

Our result shows that the measurement of double-diffractive double-elastic production of η_c should be possible. However, one should remember about very small branching fractions for different decay channels of η_c. It is not clear to us at present if the missing mass technique could be used at the Fermilab Tevatron. This would help to avoid the small branching fraction problem. The results obtained with different UGDFs differ significantly. Any measurement of the reaction would be then very interesting to estimate (or limit) UGDFs in the nonperturbative region.

IV. DISCUSSION AND CONCLUSIONS

For the first time in the literature, we have calculated exclusive production of η' meson in high-energy $pp \to p\eta' p$ collisions within the formalism of unintegrated gluon distributions. This type of reaction exhibits an incredible sensitivity to the choice of UGDF, which makes precise predictions rather difficult. Measurements of this reaction, however, would help to limit or even pin down the UGDFs in the nonperturbative region of small gluon transverse momenta k_t where these objects cannot be obtained as a

solution of any perturbative evolution equation, but must be rather modeled. The usual procedure is to extrapolate the perturbative regime via a smooth parametrization. For most of inclusive reactions the details of such a procedure are not essential. In contrast, for the reaction discussed here the extrapolation is crucial.

In contrast to diffractive Higgs production, in the case of light meson production the main contribution to the amplitude comes from the region of very small gluon transverse momenta and very small longitudinal momentum fractions. In this case application of Khoze-Martin-Ryskin UGDFs seems not to be justified and we have to rely on UGDFs constructed for this region.

The existing models of UGDFs predict cross section much smaller than the one obtained by the WA102 collaboration at the center-of-mass energy $W = 29.1$ GeV. This may signal presence of subleading reggeons at the energy of the WA102 experiment or suggest a modificaction of UGDFs in the nonperturbative region of very small transverse momenta. Experiments on exclusive central production of η' at RHIC, Tevatron and LHC would certainly help in disentangling the problem. With some cuts on ξ_1, ξ_2, t_1 and t_2 the reaction under consideration can be measured at the Fermilab Tevatron [30]. An exact evaluation of the experimental cross section for the Tevatron will be presented elsewhere.

A reasonable description of the WA102 total cross section can be obtained with UGDF obtained by Gaussian smearing of collinear gluon distributions and rather small value of the smearing parameter $\sigma_0 \sim 0.2$–0.3 GeV, clearly pointing to a nonperturbative effect. If the parameter σ_0 is adjusted to the total cross section a reasonable description of the $d\sigma/dx_F$ around $|x_F| < 0.2$ is obtained simultaneously. This was not possible with the Regge-like (two-pomeron exchange) description of the reaction [11] which produced distribution too much peaked at $x_F \approx 0$. However, our approach gives somewhat too much skewed (asymmetric around $\Phi = \pi/2$) distribution in relative azimuthal angle between outgoing protons compared to the WA102 data. This model gives definite predictions at larger energies where the contribution of subleading reggeons should be negligible. Experimental data at different collision energies would verify the solution and shed more light on the dynamics of the η' meson production. At present the Tevatron apparatus could be used.

Measurement at lower energies would be also interesting. Natural possibilities would be FAIR at GSI and J-PARC at Tokai. Such data could shed more light on the role of subleading reggeons which seems important in understanding the WA102 data.

Because of a nonlocality of the loop integral our model leads to sizeable deviations from the $\sin^2\Phi$ dependence (predicted in the models of one-step fusion of two vector objects).

The $\gamma^*\gamma^*$ fusion gives the cross section of the order of a fraction of nb at the WA102 energy $W = 29.1$ GeV, i.e. much less than 1% of the measured cross section. The $\gamma^*\gamma^*$ fusion may be of some importance only at extremely small four-momentum transfers squared. In addition it can interfere with the QCD mechanism, which is similar to the familiar Coulomb-nuclear interference for charged hadron elastic scattering.

Finally we have presented results for exclusive double elastic η_c production. Similar cross sections as for η' production were obtained. Also in this case the results depend strongly on the choice of UGDF.

In the present calculations we have calculated only so-called bare amplitudes which are subjected to absorption corrections. The absorption effects lead usually to an energy-dependent damping of the cross section for exclusive channels. At the energy of the WA102 experiment $W = 29.1$ GeV the damping factor is expected to be of the order 5–10 [6] and should increase with rising initial energy. A detailed analysis of absorption effects is left for a future separate study.

ACKNOWLEDGMENTS

We are indebted to Kolya Kochelev and Andrey Vinnikov for providing us the WA102 data and Paweł Moskal for providing us low-energy data. We also thank Christophe Royon for a discussion about possibilities to measure the $pp \to p\eta' p$ reaction at the Fermilab Tevatron. We are grateful to Alexei Kaidalov, Valery Khoze and Roland Kirschner for a discussion on the applicability of QCD factorization to double diffraction. This work was partially supported by the grant of the Polish Ministry of Scientific Research and Information Technology number 1 P03B 028 28 and by RFBR grant No. 06-02-16215.

[1] A. Schäfer, O. Nachtmann, and R. Schöpf, Phys. Lett. B **249**, 331 (1990).
[2] A. Białas and P. V. Landshoff, Phys. Lett. B **256**, 540 (1991).
[3] J.-R. Cudell and O. F. Hernandez, Nucl. Phys. **B471**, 471 (1996).
[4] V. A. Khoze, A. D. Martin, and M. G. Ryskin, Phys. Lett. B **401**, 330 (1997).
[5] V. A. Khoze, A. D. Martin, and M. G. Ryskin, Eur. Phys. J. C **23**, 311 (2002).
[6] A. B. Kaidalov, V. A. Khoze, A. D. Martin, and M. G. Ryskin, Eur. Phys. J. C **31**, 387 (2003).

[7] A. B. Kaidalov, V. A. Khoze, A. D. Martin, and M. G. Ryskin, Eur. Phys. J. C **33**, 261 (2004).
[8] P. Moskal *et al.* (COSY11 collaboration), Phys. Rev. Lett. **80**, 3202 (1998); Phys. Lett. B **474**, 416 (2000); **482**, 356 (2000).
[9] F. Balestra *et al.* (DISTO collaboration), Phys. Lett. B **491**, 29 (2000).
[10] K. Nakayama and H. Haberzettl, Phys. Rev. C **69**, 065212 (2004).
[11] N. I. Kochelev, T. Morii, and A. V. Vinnikov, Phys. Lett. B **457**, 202 (1999).
[12] D. Barberis *et al.* (WA102 collaboration), Phys. Lett. B **422**, 399 (1998).
[13] F. E. Close and G. A. Schuler, Phys. Lett. B **464**, 279 (1999); Phys. Lett. B **464**, 279 (1999).
[14] J. Forshaw, hep-ph/0508274.
[15] V. A. Khoze, A. D. Martin, M. G. Ryskin, and W. J. Stirling, Eur. Phys. J. C **35**, 211 (2004).
[16] B. Pire, J. Soffer, and O. Teryaev, Eur. Phys. J. C **8**, 103 (1999); X. Artru, M. Elchikh, J.-M. Richard, J, Soffer, and O. Teryaev (unpublished).
[17] J. Bartels, S. Bondarenko, K. Kutak, and L. Motyka, Phys. Rev. D **73**, 093004 (2006).
[18] P. Castoldi, R. Escribano, and J.-M. Frere, Phys. Lett. B **425**, 359 (1998).
[19] M. Diehl, P. Kroll, and C. Vogt, Eur. Phys. J. C **22**, 439 (2001); Eur. Phys. J. C **22**, 439 (2001).
[20] J. Gronberg *et al.* (CLEO collaboration), Phys. Rev. D **57**, 33 (1998).
[21] A. Donnachie and P. V. Landshoff, Phys. Lett. B **185**, 403 (1987); **191**, 309 (1987); Nucl. Phys. **B303**, 634 (1988).
[22] M. Łuszczak and A. Szczurek, Phys. Rev. D **73**, 054028 (2006).
[23] K. Golec-Biernat and M. Wüsthoff, Phys. Rev. D **60**, 114023 (1999).
[24] D. Kharzeev and E. Levin, Phys. Lett. B **523**, 79 (2001).
[25] E. A. Kuraev, L. N. Lipatov, and V. S. Fadin, Sov. Phys. JETP **45**, 199 (1977); Ya. Ya. Balitskij and L. N. Lipatov, Sov. J. Nucl. Phys. **28**, 822 (1978).
[26] M. Łuszczak and A. Szczurek, Eur. Phys. J. C **46**, 123 (2006).
[27] L. Lonnblad and M. Sjödahl, J. High Energy Phys. 05 (2005) 038; 02 (2004) 042.
[28] M. A. Kimber, A. D. Martin, and M. G. Ryskin, Eur. Phys. J. C **12**, 655 (2000); Phys. Rev. D **63**, 114027 (2001).
[29] M. Glück, E. Reya, and A. Vogt, Z. Phys. C **67**, 433 (1995).
[30] C. Royon (private communication).